Fiske steps and hysteresis in $YBa_2Cu_3O_7$ grain boundary Josephson junctions: Structural information of the barrier by means of a nondestructive approach

M. A. Navacerrada,[1] M. L. Lucía,[2,a)] F. Sánchez-Quesada,[2] and E. Sarnelli[3]
[1]*Dpto. Física e Instalaciones, Escuela de Arquitectura, Universidad Politécnica de Madrid, Avda. Juan de Herrera, 4, 28040 Madrid, Spain*
[2]*Dpto. Física Aplicada III, Facultad de CC. Físicas, Universidad Complutense, Avda. Complutense, s/n, 28040 Madrid, Spain*
[3]*Istituto di Cibernetica, "E. Caianiello" del CNR, Via Campi Flegrei, 34, 80078 Pozzuoli, Italy*

(Received 19 May 2008; accepted 25 October 2008; published online 10 December 2008)

A deep analysis of the current-voltage (*I-V*) characteristics of $YBa_2Cu_3O_7$ grain boundary Josephson junctions (GBJJs) allows us to go much farther than the usual calculus of the transport parameters. It is possible to construct a structural image of the barrier by an exhaustive and complementary analysis of both transport and electromagnetic parameters obtained from *I-V* curves. For such an approach, we have chosen the following three representative bicrystalline geometries: 24° [001] asymmetric, 45° [100] asymmetric, and 24° [001] symmetric +45° [100] asymmetric. The dependence of the product I_CR_N on the junction normal resistance is of the $I_CR_N^{-1}$ type pointing to a SNINS model (S denotes superconductor, I denotes insulator, and N denotes normal metal) for all our GBJJs. A satisfactory explanation of the discrepancy of the capacitance of the barrier estimated from Fiske resonance positions and hysteresis in the *I-V* curves needs of such a model. Moreover an estimation of the length of the normal regions adjacent to the crystallographic barrier can be made. This comparative analysis is presented in order to extract interesting information about the particular transport mechanisms involved in these GBJJs. © *2008 American Institute of Physics*. [DOI: 10.1063/1.3040083]

I. INTRODUCTION

The most studied $YBa_2Cu_3O_7$ (YBCO) grain boundary Josephson junctions (GBJJs) are fabricated on both [001] tilt symmetric and asymmetric bicrystalline substrates, respectively. However, in the past years, YBCO GBJJs fabricated on [100] substrates have also been investigated.[1–5] The structure of the barrier of YBCO GBJJs fabricated on bicrystals depends on many factors such as the misorientation angle and the orientation of the interface plane with respect to the crystallographic axes. In general, these YBCO GBs present a complicated microstructure with a meandering around the substrate bicrystal GB and nanofacets with various local misorientations.[6] This information has been mainly derived through transmission electron microscopy techniques.[1,2] Taking into account that these techniques are destructive tests, any structural information directly derived from the analysis of the electromagnetic and transport parameters of the YBCO barriers would be very useful. For instance, the observation of electromagnetic resonances in the GB has confirmed its electrically insulating nature, at least partially.[7] Moreover, the low carrier density of the cuprates in combination with the large dielectric constant is expected to lead to a significant band bending and the formation of space-charge layers at interfaces.[8,9]

We have previously published several works showing the power of the electromagnetic parameters to reveal interesting insights on the nature of the barrier and to corroborate the information deduced from the analysis of transport parameters.[10–12] The results deduced in Ref. 10 were based on the analysis of the capacitance (*C*) associated with the barrier determined from both Fiske steps resonances and hysteresis of the current-voltage (*I-V*) curves of the junctions. Some authors have shown that in the case of YBCO GBJJs fabricated on 24° and 36° [001] bicrystalline substrates,[13,14] the capacitance calculated from the Fiske resonances correlates well with that one determined from the hysteresis present in the *I-V* curves. However, we have observed a discrepancy in the case of GBJJs fabricated on 45° [100] bicrystals as described in Ref. 10. We believe that this discrepancy is related to the fact that different regions of the GB contribute to the capacitance values estimated in the two different methods. The small *C* values deduced from the *I-V* hysteresis point to a serial contribution of the regions adjacent to the GB. This result makes it reasonable to describe these junctions within a tunnel model rather than in a filamentary framework.[10,12]

To perform the analysis, we propose to calculate the relative dielectric constant to the crystallographic barrier thickness ratio (ε_r/t) for each junction width *w*.[15] Each ε_r/t is derived by measuring the voltage of the Fiske steps

$$V_n = \frac{n\phi_0\bar{c}}{2w}, \tag{1}$$

where *n* is the resonance number, $\bar{c}$ is the Swihart velocity, and ϕ_0 is the flux quantum.[15] Once $\bar{c}$ is deduced, ε_r/t ratio is calculated by using the expression $\bar{c}=[c_0(t/\varepsilon_r d)^{1/2}]$, where c_0

a)Electronic mail: mllucia@fis.ucm.es.

 © 2008 American Institute of Physics

Downloaded 30 Jun 2009 to 147.96.21.108. Redistribution subject to AIP license or copyright; see http://jap.aip.org/jap/copyright.jsp

is the vacuum light velocity and d is the effective magnetic junction length. According to expression (1), by varying w, we are actually modifying V_n and so the resonant frequency $f_n = V_n/\phi_0$. In this way, we are able to explore in detail the dispersion relation $\varepsilon_r(f_n)$, which is essentially the relation ε_r versus frequency (ω), where ω is the frequency of the electromagnetic wave propagating in the junctions. This analysis was carried out for different bicrystal geometries ([001] tilt, [100] tilt, and [100] tilt-tilt), which are known to have different barrier structures and transport mechanisms. For all the geometries, the proximity to a resonance in the dielectric response was analyzed. The resonance frequency ω_0 and damping parameter γ were explored. They show a tendency to a semiconductive behavior with the increase in the misorientation angle of the bicrystalline substrate. From a physical point of view, this frequency dependence suggests that the YBCO GBJJs cannot be modeled as a perfect dielectric cavity and the contribution of electrical losses must be considered. The consistency of this model for the dielectric constant is proven by the accordance with the results deduced from the electrical characterization performed on YBCO [001] tilt and [100] tilt GBJJs.

The aim of the present work is to show that it is possible to create a structural image of the YBCO GBJJs by means of a nondestructive approach, which is the calculus and study of electromagnetic and transport parameters. To achieve this target, a deep exploration of the discrepancy observed in the C values deduced from Fiske steps and hysteresis I-V curves mainly for [100] bicrystalline geometries is necessary. In this line, we present in this work the results of a different geometry, 24° [001] symmetric +45° [100] asymmetric GBJJs. Also, we corroborate that such a discrepancy does not take place in 24° [001] asymmetric GBJJs. We explore a SNINS model (S denotes superconductor, I denotes insulator, and N denotes normal metal) for the barriers, and we estimate the length of the normal N regions in all our samples. In the calculus of this length, it is necessary to use a dielectric constant value that correctly considers the microstructure of the barrier. One of the contributions of this work is the deduction of this value for the dielectric constant from the dispersion relation.

II. EXPERIMENTAL

In this paper, we have chosen three following representative geometries: 24° [001] asymmetric, 45° [100] asymmetric, and 24° [001] symmetric +45° [100] asymmetric. The reason for this choice is clear and it is because the former two geometries have been extensively studied in the literature, so it would be very interesting to investigate and compare the properties of these junctions with the GBJJs fabricated on substrates tilted around both [100] and [001] axis. The scheme of Fig. 1 illustrates the different bicrystalline orientations. The misorientation angles for the three geometrical configurations we have analyzed are indicated in Table I. The [100] tilt and [100] tilt-tilt bicrystal geometries are of the "valley" type, being the [001] axis tilted toward the GB.

80 nm thick YBCO films were epitaxially grown in a high pressure (3.4 mbar) dc sputtering system in pure oxygen atmosphere. In the deposition process, the substrate temperature is 900 °C. Electrodes show critical temperatures in the range of 89.5–91 K, transition widths smaller than 0.2 K, and critical current densities higher than 10^6 A/cm^2 at 77 K. The accurate control of the film growth process in our sputtering system has been previously demonstrated.[10–12] 100 nm thick gold layers were deposited on the samples for making low contact resistance paths. Films were patterned obtaining junction widths ranging between 4 and 20 μm by Ar ion milling, cooling the sample holder down to −50 °C. The I-V characteristic of the samples have been measured using homemade electronics characterized by a current amplifier showing 0.1 nA/Hz$^{1/2}$ current noise, and a voltage differential amplifier with 7 nV/Hz$^{1/2}$ output voltage noise at 10 Hz, respectively. Moreover, the junction leads are filtered by individuals cryogenic π filters (one filter per wire), located close to the sample, with a cutoff frequency of about 10 kHz. This guarantees that no high-frequency contribution (rf signals) coming from the external environment is reaching the junction. Considering the extremely low values of the junction capacitances, of the order of several femtofarads, in order to guarantee that the external circuit does not influence the measurements, the effect of stray capacitances and/or inductances of wires connecting the junction pads to the cryogenic filters is also worthy to be analyzed. As a rough calculation, the resonance frequency related to the external circuit is of the order of 30 MHz. If the total capacitance of the circuit would be the one associated with the wires, this would induce a current step in the I-V characteristic at the voltage $V \approx 2$ μV that is lower than the range we are dealing with. It means that the capacitance we have measured (see next paragraph) by using current steps is completely due to the junction.

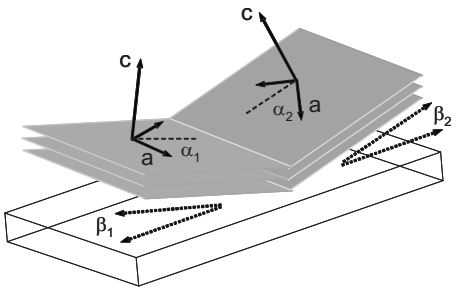

FIG. 1. Schematic representation of the [001] and [100] bicrystal orientations. The [001] axis of the electrodes are tilted in plane by angles α_1 and α_2. The case $\alpha_1=\alpha_2=0$ corresponds to a [100] tilt boundary. The left (right) [001] axis is tilted by an angle β_1 (β_2). The case $\beta_1=\beta_2=0$ corresponds to a [001] tilt boundary.

TABLE I. Values of the bicrystal α and β misorientation angles for all our GBJJs.

Bicrystal geometry	α_1	α_2	β_1	β_2
[001] tilt: 24° [001] asymmetric	24°	0	0	0
[100] tilt: 45° [100] asymmetric	0	0	0	45°
[100] tilt-tilt: 24° [001] symmetric +45° [100] asymmetric	12°	12°	0	45°

Downloaded 30 Jun 2009 to 147.96.21.108. Redistribution subject to AIP license or copyright; see http://jap.aip.org/jap/copyright.jsp

TABLE II. $I_C R_N$ products as a function of the junction width (w).

Junction width w (μm)	24° [001] $I_C R_N$ (mV)	45° [100] $I_C R_N$ (mV)	24°[001]+45°[100] $I_C R_N$ (mV)
20	2.4	6.1	5.9
20	2.3	5.5	2.7
10	2.2	3.2	2.9
10	2.4	4.8	3.2
4	2.6	1.7	4.9
4	1.9	5.1	1.1

The dewar is shielded by an external 1 cm thick aluminum box surrounding three internal micrometal cylinders. Moreover, a double shield made of two concentric cryoperm and lead cylinders surrounds the probe. Junctions are mounted under vacuum and the thermal contact to the cryogenic bath is made by a partial pressure of several Torr of helium gas inside the vacuum chamber. Finally, an external magnetic field may be applied through a solenoid with multiturn coils positioned inside the double shield. The I-V curves for different values of applied magnetic field parallel to the GB plane have been measured.

III. RESULTS AND DISCUSSION

A. Transport parameters: I_C and R_N

In Table II, we show some representative examples of the $I_C R_N$ product values deduced from the I-V curves for three w of our junctions. The values of $I_C R_N$ in YBCO [100] tilt and [100] tilt-tilt junctions are generally higher than the values measured in YBCO [001] tilt junctions. The possibility to have Josephson junctions with a high $I_C R_N$ product could be of interest for the fabrication of different electronic devices as dc superconducting quantum interference devices and high frequency superconductive devices. Following with the analysis, such product is almost constant in the case of our 24° [001] tilt junctions. This points to a high quality of the samples fabricated and to the filamentary model as the transport mechanism for this geometry.[16] Presumably, a larger faceting is achieved in [100] tilt and [100] tilt-tilt junctions rather than in 24° [001] tilt junctions. The scattering observed in the $I_C R_N$ product for the former geometries has been explained taking into account both a tunneling behavior and a d-wave effect.[3]

In this line, the dependence of the critical current on the junction resistance has also been investigated. As it can be seen in Fig. 2, data corresponding to our three bicrystalline geometries are distributed along a potential dependence of the type $I_C R_N^{-a}$ being the parameter a of the order of 1.17. A value of $a=1$ is also expected for SNINS structures,[17] other than in the case of pure SIS tunnel junctions.[3] In principle, this argument is only valid when the barrier is thin (less than 18 nm). Nevertheless, it is remarkable that all the data fit very well to such a relation so in the following we will make use of this description of the barrier.

B. Capacitance

The length of the normal region at both sides of the SNINS barrier can be obtained from the analysis of the junction capacitance. The capacitance per unit area associated with the barrier (C/A) has been determined both from Fiske steps resonances and hysteresis of the I-V curves. In this discussion, particular care has been taken in order to eliminate possible sources of error.[11,12] The dielectric response of the strontium titanate substrate is frequency dependent and at low frequencies the relative dielectric constant can be large (below 200 GHz at 4.2 K).[18] If such a frequency range is reached, the substrate may affect the capacitance determination of the barrier. Then it is compulsory to ensure that the capacitances calculated from Fiske steps and the hysteresis observed in the I-V curves are associated only to the GB. Moreover, it is important to point out that the position of the Fiske step $n=1$ is always over the approximated limit of 0.3 mV fixed by Ransley *et al.*[19] These authors claim that over this voltage limit, the frequency is large enough so that the dielectric contribution of the substrate is low. The same authors have shown that at low temperature, the substrate contributes to the capacitance calculated by means of the I-V curve hysteresis at return voltages below 0.25 mV, and in our case this limit is exceeded.

In the analysis of the dielectric response of the barrier, $\bar{c}$ has been determined by the position of the Fiske step V_1 ($n=1$) and ε_r/t ratios are calculated using expression (1). As an example, in Fig. 3, we show two I-V characteristics where the positions of Fiske steps are indicated. Fiske steps can be

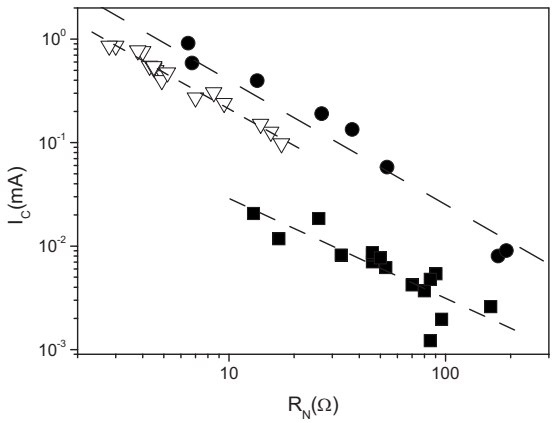

FIG. 2. Plot of the critical current (I_C) vs normal resistance (R_N) for our three bicrystalline geometries: 24° [001] asymmetric (▽), 45° [100] asymmetric (●), and 24° [001] symmetric +45° [100] asymmetric (■).

Downloaded 30 Jun 2009 to 147.96.21.108. Redistribution subject to AIP license or copyright; see http://jap.aip.org/jap/copyright.jsp

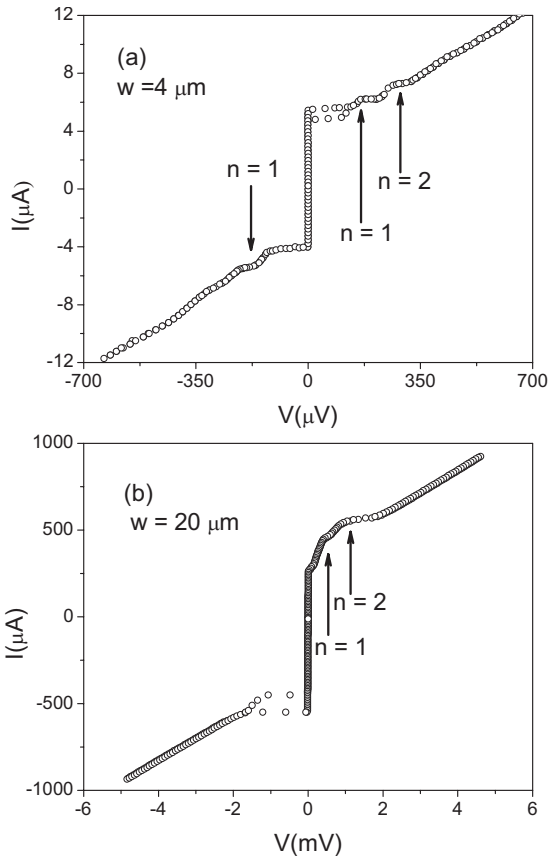

FIG. 3. *I-V* curves corresponding to (a) 24° [001] symmetric +45° [100] asymmetric (B=0.8 G) and (b) 45° [100] asymmetric (B=1 G) YBCO GBJJs. The widths of the junctions and the positions of Fiske steps n=1 and n=2 are indicated in the figures.

easily identified because of the dependence of their intensity on the magnetic field applied parallel to the GB plane (see Fig. 4). More evidences of these dependences can be seen in Ref. 12. Since the thickness δ of our films is always smaller than the London penetration depth (λ_L), d has to be calculated using the expression $\lambda=\lambda_L \coth(\delta/\lambda_L)$.[7] The whole procedure is repeated for each substrate geometry and for each w, using the value λ_L=140 nm. The C/A ratios are calculated as $\varepsilon_r\varepsilon_0/t$.

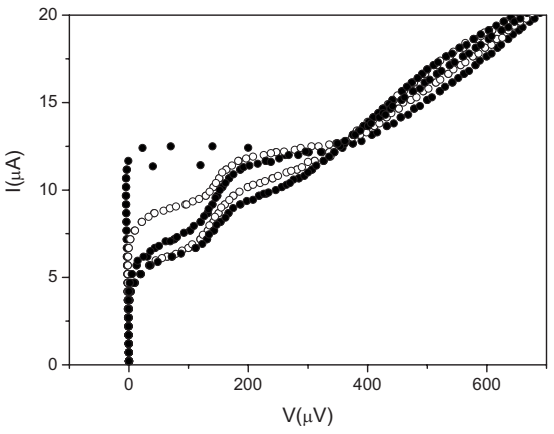

FIG. 4. *I-V* curves corresponding to a 24° [001] symmetric +45° [100] asymmetric YBCO GBJJ for different magnetic fields applied parallel to the GB plane, ranging between 0 and 10 G. We have used alternatively open and bold symbols for the sake of clarity.

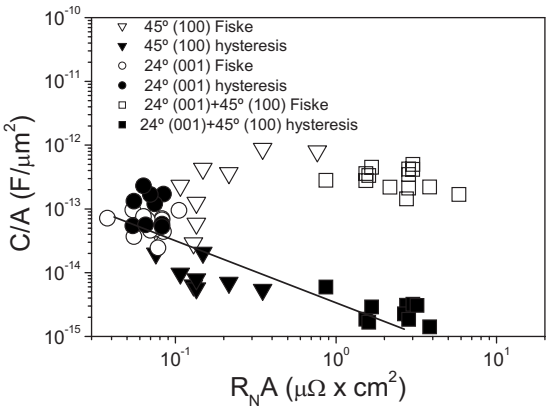

FIG. 5. Dependence of junction capacitance per unit area (C/A) with junction resistance (R_NA). Open symbols correspond to C/A calculated from Fiske step voltage positions and bold symbols correspond to C/A calculated from *I-V* curve hysteresis.

For both [100] tilt and [100] tilt-tilt GBJJs, the three following different behaviors have been identified:[20] (a) *I-V* curves following the resistively shunted junction (RSJ) model,[7] (b) *I-V* curves showing multiple current steps,[21] and (c) *I-V* curves showing a clearly displaced linear slope, typically encountered in very long tunnel junctions.[7] Then, concerning the C/A values calculated by means of the hysteresis observed in the *I-V* curves, only a limited number of *I-V* curves of YBCO [100] tilt and [100] tilt-tilt GBJJs are well described by the RSJ model. However, we consider it appropriate to obtain the McCumber parameter $\beta_C=2\pi I_C R_N^2 C/\phi_0$ for the calculus of C from Zappe's approximation $\beta_C=(2-(\pi-2)\alpha)/\alpha^2$ in terms of the ratio $\alpha=I_R/I_C$ of the return current I_R to I_C.[22] In all cases, the hysteresis is large enough to extract the I_C and I_R values in order to calculate β_C. All our β_C values calculated using this approximation are higher than unity, in agreement with the established criteria to observe hysteresis in the *I-V* curves.[7]

Variations in the C/A ratio with R_NA for the three bicrystalline geometries are shown in Fig. 5. The C/A values obtained from Fiske step positions correlate well with the ones determined from the hysteresis only in the case of [001] tilt junctions. For the [100] tilt and [100] tilt-tilt bicrystalline geometries, the values deduced from Fiske resonances are higher than those deduced from hysteresis. The experimental accuracy in voltage and current measurements lead to an error in the evaluation of the capacitance, using both methods, in the range of 10^{-16}–10^{-18} F/μm^2. This range is far below the differences between Fiske and hysteresis capacitances shown in Fig. 5 for any bicrystalline geometry (not lower than 10^{-14} F/μm^2). Then, in the following, we can perform a correct quantitative comparison of these capacitances. Data relative to [001] tilt substrate follow the power law $(C/A)\alpha(R_NA)^{-1}$.[23] This behavior is common to many [001] tilt GBJJs of different misorientation angles, and it is presented as consistent with the phenomenological filamentary model to describe the transport mechanism across the barrier.[16,23]

We believe that the discrepancy observed between both methods in the case of YBCO [100] tilt and [100] tilt-tilt GBJJs is related to the fact that different regions of the GB

Downloaded 30 Jun 2009 to 147.96.21.108. Redistribution subject to AIP license or copyright; see http://jap.aip.org/jap/copyright.jsp

contribute to C/A. Indeed, Fiske steps are a consequence of an interaction of the Josephson current with resonant modes of the barrier. The propagation direction of the resonant modes is along the longitudinal direction of the barrier regarded as a transmission line and normal to the Josephson current. In this sense, as we have previously suggested, it is reasonable to assume that only the most oxygen deficient regions of the barrier, very close to the crystallographic GB, would form the effective dielectric medium supporting the wave propagation. We believe that the calculated ε_r/t ratio from Fiske steps is only related to the resonant cavity, so the insulating region inside the SNINS barrier. The smaller C values derived from hysteresis are the effect of the serial contribution of the different regions adjacent to the crystallographic GB, in our case the normal regions N deduced from the analysis of the transport parameters. The length of these N regions can be estimated for each junction assuming the serial contribution of three layers, the crystallographic GB, and the adjacent regions, by means of the expression

$$\frac{1}{C_{\text{hysteresis}}} = \frac{1}{C_t} + \frac{2}{C_{\text{adjacent}}}, \tag{2}$$

where C_t is the value associated with the GB or insulating regions and determined from the Fiske resonances and C_{adjacent} represents the capacitance associated with the adjacent regions. Using $C_{\text{adjacent}}=\varepsilon_r'\varepsilon_0/L$, where ε_r' is the relative dielectric constant of the N layers, the value of L can be estimated for each junction width w. For the determination of ε_r', the value given by the expression

$$\varepsilon_r' = 1 + \frac{NQ^2}{m\varepsilon_0\omega_0^2} \tag{3}$$

has been used, where N is the number of atoms per volume unit, Q is the charge carrier per unit cell, and m is the mass of free electrons. Previously we have explored the proximity to a resonance in the dielectric response of the barrier. In that analysis, the values of NQ^2/mt, t, and ω_0 are derived from the fitting of the experimental dispersion relation $\varepsilon_r(\omega)$ to the theoretical expression for a resonance in the frequency response of a dielectric constant of a material.[11,12] An average mean value $\varepsilon_r=28$ has been obtained by means of expression (3) for our geometries. In several works published in the literature ε_r' values ranging between 5 and 10 have been assumed as estimated for oxygen deficient YBCO.[24] We believe that besides oxygen deficiency, structural disorder is present in these regions constituting the structural transition from the disordered barrier to the good superconducting regions of the electrodes. This structural disorder induced in the YBCO lattice by the GB is responsible for modeling the crystallographic GB as a dielectric medium with losses. In this sense, we consider more appropriated for the calculus of L the low frequency dielectric constant value. In Table III, we have reported values derived for L for some representative junctions of the three bicrystalline geometries studied.

TABLE III. Length of the normal region N adjacent to the crystallographic GB for some representative junctions.

Junction width w (μm)	24° [001] L (nm)	45° [100] L (nm)	24°[001]+45°[100] L (nm)
20	0	3.7	54.8
20	1.5	19.5	39.0
10	1	14.6	38.6
10	1.9	15.2	42.2
4	0	17.0	42.2
4	0	5.5	20.3

C. Transport mechanism

As shown in Table III, the L values range between 0 and 2 nm in the case of [001] tilt junctions. We believe that this result is in accordance with a SNINS barrier description, and the transport mechanism can be analyzed in the context of the filamentary model. In this model, the barrier is regarded as a disordered dielectric medium but with a high density of superconducting filaments. Taking into account the total width of the SNINS barrier, superconducting filaments can exist bridging the GB and supporting the supercurrent.[16,23]

In the case of YBCO [100] tilt and [100] tilt-tilt junctions, the following two aspects are remarkable: (1) the dispersion in the L values in junctions fabricated even on the same bicrystalline substrate and (2) the magnitude of such values. It seems clear that the complex electronic behavior of the high superconducting materials also reflects in the properties of their interfaces. In this sense, we believe that our data are revealing important information about the structure and transport mechanism in these two geometries of YBCO GBJJs.

Concerning the dispersion in the L values, we believe that it is a consequence of the faceting of the barrier plane caused during film growth by the competition of grain orientations along the interface. In the following, we assume a random distribution of facet widths and angles for each bicrystalline substrate. This distribution is unique to each junction, depending strongly on the angle and uniformity of the substrate GB interface and the growth kinetics of the deposited cuprate films. From atomic force microscopy images, it is estimated that typical meandering widths range from 5 to 100 nm and a wide range of angles as observed in [100] tilt junctions.[1,2] In this sense, the structure of the barrier can be very different from one junction to another fabricated on the same bicrystalline substrate. So, the dispersion observed is reasonable as a measure of the faceting of the barrier.

Going into the structure of the junction barrier, in principle, this situation may seem strange because of the high L values calculated. In the band-bending model,[8,9] the barrier is considered as consisting of three layers, the structurally distorted interface in the middle and two adjacent charge-depleted layers of undistorted material. However, the band bending is proposed to take place on the length scale of the YBCO lattice constant. In this line, we believe that the presence of these long regions more than band bending are related to the fact that relative positions of atoms (so bond lengths, valence of atoms, and number of charge carrier) are modified by strain in the vicinity of the GB.

Following with the analysis of the transport mechanism, in the high voltage region, the I-V curves of [100] tilt and [100] tilt-tilt junctions show a parabolic behavior. Figure 6

Downloaded 30 Jun 2009 to 147.96.21.108. Redistribution subject to AIP license or copyright; see http://jap.aip.org/jap/copyright.jsp

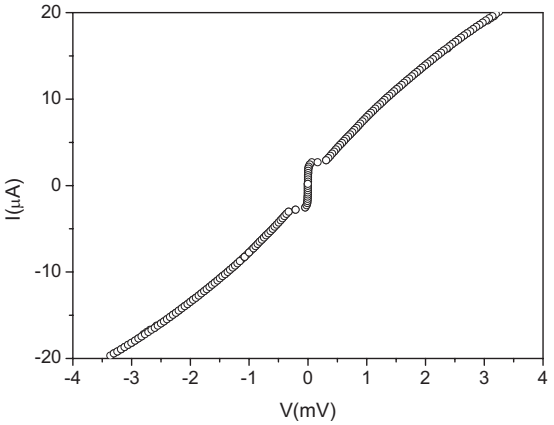

FIG. 6. *I-V* characteristic of a 24° [001] symmetric +45° [100] asymmetric junction where a parabolic behavior is observed.

shows an example of such a behavior corresponding to a [100] tilt-tilt junction. This behavior has been reported and this nonlinearity together with the scaling relation of the I_cR_n product versus J_c observed in these junctions seems to suggest the presence of a tunneling barrier.[3,24,25] However, considering the lengths calculated for the normal regions in our samples, it seems reasonable that other mechanisms may also contribute to the electrical transport in these GBJJs. We believe that a consequence of the disorder induced by the GB is the presence of localized states.[26,27] Our results seem to indicate the need to incorporate also the role of these localized states into the tunneling model responsible for the transport mechanism in these junctions, although a definitive confirmation in this direction can be obtained only after noise experiments. In fact, some authors claim that different local atomic GB structures with different densities of localized states may be responsible for the higher I_CR_N product values of the [100] tilt boundary junctions.[1,2] Junctions based on YBCO/PBCO/YBCO, where the thickness of the barrier is higher than 20 nm, show a SNINS behavior. A nonconventional theory based on either tunneling or proximity effect has given a satisfactory explanation for the mechanism of Josephson coupling through the considerably thick PBCO barrier (up to several tens of nanometers). Resonant tunneling of Cooper pairs through localized states with long localization length has been proposed as a possible origin of Josephson coupling in these junctions.[28,29] On the other hand for interfaces between *d*-wave superconductors, the orientation of the superconductors with respect to the junction is an important parameter controlling the junction properties. Likewise, also the roughness of the barrier is a parameter much more important than in conventional junctions.[5]

IV. CONCLUSIONS

In summary, we have explored the possibility to create a structural picture of the barrier of YBCO GBJJs by means of a nondestructive approach such as the study of transport and electromagnetic parameters. On the one hand, the analysis of the I_C and R_N parameters reveals a SNINS type barrier for the [100] junctions, in agreement with the tunneling behavior shown in previous experiments. On the contrary, [001] GBJJs have confirmed a filamentary transport mechanism of the supercurrent. On the other hand, the lengths of the normal regions (L) have been estimated from the discrepancy observed in the C values derived from the Fiske resonance voltage positions and the *I-V* curve hysteresis. The L values are much smaller in the case of [001] tilt junctions while ranging between 4 and 55 nm for the [100] tilt and [100] tilt-tilt junctions. This dispersion in the L values for these two bicrystalline geometries is a consequence of the typical meandering of the barriers in these YBCO GBJJs, as observed by electron microscopy techniques.

[1] U. Poppe, Y. Y. Divin, M. I. Faley, J. S. Wu, C. L. Jia, P. Shadrin, and K. Urban, IEEE Trans. Appl. Supercond. **11**, 3768 (2001).
[2] Y. Y. Divin, U. Poppe, C. L. Jia, P. Shadrin, and K. Urban, Physica C **372–376**, 115 (2002).
[3] E. Sarnelli, G. Testa, D. Crimaldi, A. Monaco, and M. A. Navacerrada, Supercond. Sci. Technol. **18**, L-35 (2005).
[4] M. Oishi, N. Chikumoto, J. Kato, S. Tajima and M. Otsuka, Physica C **426-431**, 79 (2005).
[5] F. Lombardi, T. Bauch, J. Johansson, K. Cedergren, T. Lindström, F. Tafuri, and E. Stepantsov, Physica C **435**, 8 (2006).
[6] H. Hilgenkamp, J. Mannhart, and B. Mayer, Phys. Rev. B **53**, 14586 (1996).
[7] A. Barone and G. Paterno, *Physics and Applications of the Josephson Effect* (Wiley, New York, 1982).
[8] H. Hilgenkamp and J. Mannhart, IEEE Trans. Appl. Supercond. **9**, 3405 (1999).
[9] J. Mannhart and H. Hilgenkamp, Physica C **317–318**, 383 (1999).
[10] M. A. Navacerrada, M. L. Lucía, L. L. Sánchez-Soto, F. Sánchez-Quesada, E. Sarnelli, and G. Testa, Phys. Rev. B **71**, 014501 (2005).
[11] M. A. Navacerrada, M. L. Lucía, L. L. Sánchez-Soto, F. Sánchez-Quesada, C. Nappi and E. Sarnelli, Phys. Rev. B **74**, 024507 (2006).
[12] M. A. Navacerrada, M. L. Lucía, L. L. Sánchez-Soto, F. Sánchez-Quesada, C. Nappi, and E. Sarnelli IEEE Trans. Appl. Supercond. **17**, 3541 (2007).
[13] P. F. McBrien, R. H. Hadfield, W. E. Booij, A. Moya, F. Kahlmann, M. G. Blamire, C. M. Pregum, and E. J. Tarte, Physica C **339**, 88 (2000).
[14] E. J. Tarte, G. A. Wagner, R. E. Somekh, F. J. Baundenbacher, P. Berghuis, and J. E. Evetts, IEEE Trans. Appl. Supercond. **7**, 3662 (1997).
[15] M. D. Fiske, Rev. Mod. Phys. **36**, 221 (1964).
[16] E. Sarnelli and G. Testa, Physica C **371**, 10 (2002).
[17] J. L. Sun and J. Gao, Phys. Rev. B **62**, 1457 (2000).
[18] R. C. Neville, B. Hoeneisen, and C. A. Mead, J. Appl. Phys. **43**, 2124 (1972).
[19] J. H. T. Ransley, P. F. McBrien, G. Burnell, E. J. Tarte, J. E. Evetts, R. R. Schulz, C. W. Schneider, A. Schmehl, H. Bielefeldt, H. Hilgenkamp, and J. Mannhart, Phys. Rev. B **70**, 104502 (2004).
[20] E. Sarnelli, G. Testa, D. Crimaldi, A. Monaco, M. Adamo, and M. A. Navacerrada, IEEE Trans. Appl. Supercond. **15**, 245 (2005).
[21] A. C. Scott and W. J. Johnson, Appl. Phys. Lett. **14**, 316 (1969).
[22] H. Zappe, J. Appl. Phys. **44**, 137 (1972).
[23] B. H. Moeckly and R. A. Buhrman, IEEE Trans. Appl. Supercond. **5**, 3414 (1995).
[24] J. Humlicek, J. Kircher, H. U. Habermeier, M. Cardona, and A. Roseler, Physica C **190**, 383 (1992).
[25] Y C. W. Schneider, S. Hembacher, G. Hammerl, R. Held, A. Schmehl, A. Weber, T. Kopp and J. Mannhart, Phys. Rev. Lett. **92**, 257003 (2004).
[26] J. Yoshida, H. Katsuno, S. Inove, and T. Nagano, Physica C **367**, 260 (2002).
[27] J. Halbritter, Phys. Rev. B **46**, 14861 (1992).
[28] J. Yoshida and T. Nagano, Phys. Rev. B **55**, 11860 (1997).
[29] J. Yoshida, S. Inove, H. Sugiyama, and T. Nagano, Physica C **335**, 226 (2000).

Downloaded 30 Jun 2009 to 147.96.21.108. Redistribution subject to AIP license or copyright; see http://jap.aip.org/jap/copyright.jsp